Solvation of the Li⁺−Br⁻−Li⁺ Triple Ion in the Gas Phase

Russell L Jarek and Seung Koo Shin*

Contribution from the Department of Chemistry, University of California, Santa Barbara, Santa Barbara, California 93106

Received June 5, 1997. Revised Manuscript Received August 19, 1997[⊗]

Abstract: The solvation of the Li⁺−Br⁻−Li⁺ triple ion with oxygen-donor Lewis bases was studied in the gas phase with use of Fourier-transform ion cyclotron resonance spectrometry. The Li⁺−Br⁻−Li⁺ triple ions were prepared in an ICR cell by matrix-assisted laser desorption ionization of a lithium bromide/dibenzo-18-crown-6-ether matrix pasted on a Teflon substrate. The stepwise solvations of LiBrLi⁺ were examined with oxygen-containing Lewis bases: 15-crown-5-ether (15C5), 12-crown-4-ether (12C4), 1,4-dioxane, 1,3-dioxane, and tetrahydrofuran (THF). Crown ethers solvate Li⁺ with loss of LiBr. 15-Crown-5-ether yields a 1:1 (15C5)·Li⁺ complex as the end product, whereas 12-crown-4-ether forms a 2:1 (12C4)₂·Li⁺ complex. On the other hand, low dielectric constant solvents, such as dioxanes and THF, solvate the Li⁺−Br⁻−Li⁺ triple ion rather than abstracting Li⁺ with loss of the neutral ion pair. The maximum coordination numbers are 3 for dioxanes and 4 for THF at 293 K. The rate constants for the stepwise solvations were measured, and the binding energies were determined from the temperature dependence of the equilibrium constants. The mechanisms of stepwise solvations are discussed in light of the structures and energetics of the 1:1 complexes of Li⁺ and LiBrLi⁺ with dioxanes and THF calculated at the Hartree−Fock level with a standard 6-311G(d,p) basis set.

The solvation of ions in the gas phase has been the focus of intensive experimental studies over the past two decades with indications that insights gained from the gas-phase results are applicable to condensed-phase processes as well.[1−3] However, gas-phase ion techniques have not provided comparable information regarding the solvation of neutral ion pairs and higher order cluster ions which can be formed in concentrated electrolyte solution.[4] At infinite dilution, a dissolved electrolyte exists in the form of the simple solvated cation and anion. As the solute concentration increases, the opposite charge ions associate to form ion pairs. When ion pairs encounter either the single ions or another ion pair as they undergo brownian motions in ionic liquid, triple ions (+ − + or − + −) or higher order clusters are formed. Although the formation of triple ions in low dielectric constant media was first proposed in 1933 by Fuoss and Kraus,[5] no experimental studies were reported to date for solvation of such ions at the molecular level in the gas phase.

The existence of triple ions in the condensed phase and the importance of their interactions with solvents are evident in recent Raman scattering studies of lithium electrolytes in polyethers.[6] Torell and co-workers suggested the formation of ion aggregates, such as Li⁺−X⁻−Li⁺ and X⁻−Li⁺−X⁻ triple ions, where X⁻ is CF₃SO₃⁻, from the concentration-dependent frequency shift in Raman spectra.[6] In nonaqueous lithium battery electrolytes it was suggested that the interactions of triple ions with O-donors in polyether complicate the temperature dependence of ion conductivity.[7,8] To provide a better understanding of solvations of triple ions in the lithium battery, the prototype Li⁺−Br⁻−Li⁺ triple ion was prepared in the gas phase and its stepwise solvations by O-donor Lewis bases were studied with Fourier-transform ion cyclotron resonance (FT-ICR) spectrometry.[9,10] In lithium batteries, poly(ethylene glycol) and poly(ethylene oxide) are commonly used as substrates, while dioxanes, tetrahydrofuran (THF), and alkyl carbonates are typical cosolvents added to balance the stability and conductivity.[7,11,12] Herein, we report the solvation kinetics and energetics of the Li⁺−Br⁻−Li⁺ triple ion with 15-crown-5-ether (15C5), 12-crown-4-ether (12C4), 1,4-dioxane (1,4-2O), 1,3-dioxane (1,3-2O), and THF.

The solvation of lithium halide salts by Lewis bases shows remarkable structural diversity in the solid state.[13−17] The triple-ion type salt-bridge structure is a common backbone linkage often encountered in the crystal structures of lithium halide complexes solvated by Lewis bases.[18−25] They form various types of complexes ranging from solvent-separated ion pairs to

(9) Comisarow, M. C.; Marshall, A. G. *Chem. Phys. Lett.* **1974,** *25,* 282−283.

(10) Marshall, A. G. *Acc. Chem. Res.* **1985,** *18,* 316−322.

(11) Appetecchi, G. B.; Croce, F.; Dautzenberg, G.; Gerace, F. *Gazz. Chim. Ital.* **1996,** *126,* 405−413.

(12) Yang, X. Q.; Lee, H. S.; Hanson, L.; McBreen, J.; Okamoto, Y. *J. Power Sources* **1995,** *54,* 198−204.

(13) Setzer, W. N.; Schleyer, P. v. R. *Adv. Organomet. Chem.* **1985,** *24,* 353−451.

(14) Seebach, D. *Angew. Chem., Int. Ed. Engl.* **1988,** *27,* 1624−1654.

(15) Mulvey, R. E. *Chem. Soc. Rev.* **1991,** *20,* 167−209.

(16) Gregory, K.; Schleyer, P. v. R.; Snaith, R. *Adv. Inorg. Chem.* **1991,** *37,* 47−142.

(17) Snaith, R.; Wright, D. S. *Lithium Chemistry: A Theoretical and Experimental Overview*; Sapse, A.-M., Schleyer, P. v. R., Ed.; Wiley: New York, 1995; pp 227−293.

(18) Hall, S. R.; Raston, C. L.; Skelton, B. W.; White, A. H. *Inorg. Chem.* **1983,** *22,* 4070−4073.

(19) Buttrus, N. H.; Eaborn, C.; Hitchcock, P. B.; Smith, J. D.; Stamper, J. G.; Sullivan, A. C. *J. Chem. Soc., Chem. Commun.* **1986,** 969−970.

(20) Amstutz, R.; Dunitz, J. D.; Laube, T.; Schweizer, W. B.; Seebach, D. *Chem. Ber.* **1986,** *119,* 434−443.

(21) Raston, C. L.; Whitaker, C. R.; White, A. H. *J. Chem. Soc., Dalton Trans* **1988,** 991−995.

(22) Barlage, H.; Jacobs, H. *Z. Anorg. Allg. Chem.* **1994,** *620,* 479−482.

(23) Raston, C. L.; Skelton, B. W.; Whitaker, C. R.; White, A. H. *Aust. J. Chem.* **1988,** *41,* 341−349.

⊗ Abstract published in *Advance ACS Abstracts,* October 15, 1997.

(1) Kebarle, P. *Ions and Ion Pairs in Organic Reactions*; Szwarc, M. Ed.; Wiley: New York, 1972; Vol. 1, pp 27−83.

(2) Aue, D. H. *Gas Phase Ion Chemistry*; Bowers, M. T., Ed.; Acedemic: New York, 1979; Vol. 2, pp 2−51.

(3) Solvation: *Faraday Discuss. Chem. Soc.* **1988,** *85,* 1−403.

(4) Smid, J. *Ions and Ion Pairs in Organic Reactions*; Szwarc, M., Ed.; Wiley: New York, 1972; Vol. 1, pp 85−151.

(5) Fuoss, R. M.; Kraus, C. A. *J. Am. Chem. Soc* **1933,** *55,* 2387−2399.

(6) Petersen, P.; Jacobsson, P.; Torell, L. M. *Electrochim. Acta* **1992,** *37,* 1495−1497.

(7) Gores, H. J.; Barthel, J. M. G. *Pure Appl. Chem.* **1995,** *67,* 919−930.

(8) Salomon, M.; Scrosati, B. *Gazz. Chim. Ital.* **1996,** *126,* 415−427.

polymers. This structural diversity is typically understood by the relative strengths of Li-donor versus Li-halide interactions, the entropy changes in complex formation, the coordination number, and the steric factors of the ligands. Though there have been extensive studies performed in the solid state, no reports were available for the intrinsic reactivities of lithium halide ions with Lewis bases in the gas phase, mainly due to the difficulty in preparing the parent ions of nonvolatile salts. Most of the previous gas-phase studies have concentrated on the solvation and reactivity of bare alkali metal ions and halide ions.[26−30] Recently, a number of novel ionization methods have been developed for the routine production of alkali-metal halide ions in the gas phase.[31,32] In this report, the matrix-assisted laser desorption ionization (MALDI) method[33−35] was employed to generate the $Li^+-Br^--Li^+$ triple ion in the ion cyclotron resonance (ICR) cell.

The present study focuses on the rates of association of $LiBrLi^+$ with O-donor Lewis bases and the coordination number in the absence of bulk solvent, which may shed light on the fundamental factors governing the diverse structures found in lithium halide−Lewis base donor complexes. Rates were measured for the stepwise solvation of $LiBrLi^+$ by O-donor Lewis bases, and binding energies of $LiBrLi^+$ by dioxanes and THF were determined from the temperature dependence of equilibrium constants. To help understand the energetics and structures of solvated complexes, *ab initio* calculations were carried out on the 1:1 complexes of Li^+ and $LiBrLi^+$ with 1,4-2O, 1,3-2O, and THF. The mechanisms of stepwise solvations are discussed in light of the theoretical structures and energetics and the experimental kinetics. The present work allows meaningful comparisons of the reactivities and structures of lithium halide complexes in the gas phase to those in the condensed phase.

Experimental Section

Experimental setups were previously described in detail.[36,37] Experimental procedures pertinent to the present study are outlined below. The FT-ICR spectrometer used in this study consisted of a 1.2 T electromagnet (Varian), a vacuum chamber with a homebuilt 1.85-in. cubic trapping ICR cell, and an FT-data system (IonSpec Inc., Omega/386) for data acquisition. There were 0.325-in. holes in the centers of receiver plates for optical access. A $^3/_8$-in.-diameter Teflon substrate was mounted on a copper plug close to the ICR cell near the center of the receiver plate. Laser radiation (308 nm) was used unfocused to

Figure 1. MALDI mass specta of (a) the isolated $LiBrLi^+$ ions and (b) $Br^-(LiBr)_n$ ($n = 1, 2$) produced from a 100:1 LiBr/dibenzo-18-crown-6-ether mixture. Each spectrum comprises 10 shot aquisitions.

desorb ions from the matrix sample pasted on the Teflon substrate. The ions trapped in the ICR cell and the neutral molecules flowing into the ICR cell were set to reach thermal equilibria in the temperature range 15−85 °C by warming up the vacuum chamber with heating pads or by cooling with air. The chamber temperature was measured at two different parts of the chamber with a type-K thermocouple.

A 100:1 molar ratio of lithium bromide salt/dibenzo-18-crown-6-ether was dissolved in a 1:1 methanol/acetonitrile solution. The mixture was sonicated for about 5 min, loaded on a Teflon substrate, and then dried in an oven at 90 °C to a visible layer. The Teflon substrate was chosen because the laser beam desorbs gaseous fluorohydrocarbons from the substrate so that the optical vacuum window remains clean. Each matrix sample lasts at least two weeks in vacuum for consecutive laser desorption experiments. Crown ether assists the laser desorption ionization process as a substrate that holds dispersed lithium salts as well as a chromopore that absorbs photons at 308 nm. Laser ablation of a LiBr pellet tends to produce higher-order cluster ions.[31,32] With a positive trapping voltage of typically 1.0 V, Li^+, $LiBrLi^+$, and $(LiBr)_2$-Li^+ were observed. When the concentration of lithium bromide was diluted to a 1:1 lithium bromide/dibenzo-18-crown-6-ether mixture, dibenzo-18-crown-6-ether-$M^+(H_2O)_n$ (M = Li, Na, and K; $n = 0, 2$) complexes were observed as the predominant species. With a negative trapping voltage, a mixture of $Br^-(LiBr)_n$ ($n = 0-4$) was observed. As an example, the mass spectra of $LiBrLi^+$ ions isolated by double resonance techniques[38] are shown in Figure 1a, and those of $Br^-(LiBr)_n$ ($n = 1, 2$) are shown in Figure 1b. Both spectra show well-resolved isotope distributions.

The background pressure in the ICR chamber was typically below 8.0×10^{-8} Torr. Gaseous samples were leaked into the ICR chamber. The sample pressures for dioxanes and THF were measured by calibrating the ion-gauge mounted in the ICR chamber against a capacitance manometer (MKS Baratron head 390HA-00010). For crown ethers, the near unit efficiency proton-transfer rates[2] were used to estimate the pressure by comparison with the Langevin collision rate constant.[39,40] For the rate constant measurements, ion signals were

(24) Rogers, R. D.; Bynum, R. V.; Atwood, J. L. *J. Crystallogr. Spectrosc. Res.* **1984**, *14*, 29−34.

(25) Gingl, F.; Hiller, W.; Strähle, J.; Borgholte, H.; Dehnicke, K. *Z. Anorg. Allg. Chem.* **1991**, *606*, 91−96.

(26) Wieting, R. D.; Staley, R. H.; Beauchamp, J. L. *J. Am. Chem. Soc.* **1975**, *97*, 924−926.

(27) Staley, R. H.; Beauchamp, J. L. *J. Am. Chem. Soc.* **1975**, *97*, 5920−5921.

(28) Chu, I. H.; Zhang, H.; Dearden, D. V. *J. Am. Chem. Soc.* **1993**, *115*, 5736−5744.

(29) Wu, H. F.; Brodbelt, J. S. *J. Am. Chem. Soc.* **1994**, *116*, 6418−6426.

(30) More, M. B.; Glendening, E. D.; Ray, D.; Feller, D.; Armentrout, P. B. *J. Phys. Chem.* **1996**, *100*, 1605−1614.

(31) Kappes, M. M.; Radi, P.; Schar, M.; Schumacher, E. *Chem. Phys. Lett.* **1985**, *113*, 243−248.

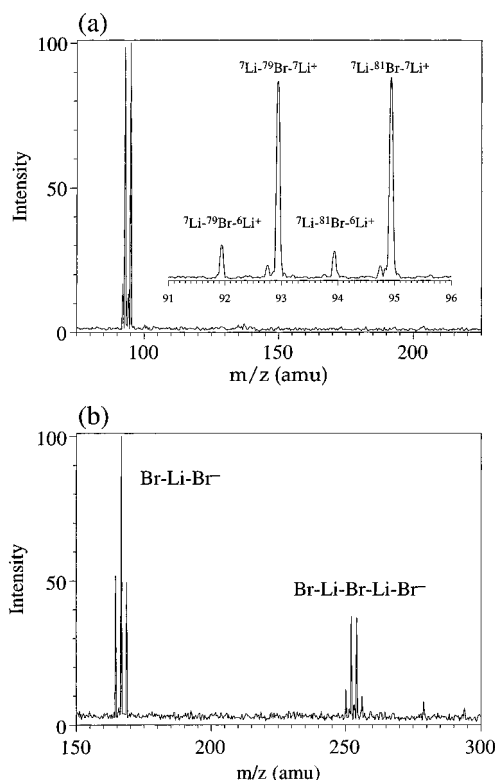(32) Whetten, R. L. *Acc. Chem. Res.* **1993**, *26*, 49−56.

(33) Ollmann, B.; Kupka, K. D.; Hillenkamp, F. *Int. J. Mass Spectrom. Ion Process* **1983**, *47*, 31−34.

(34) Karas, M.; Bachmann, D.; Bahr, U.; Hillenkamp, F. *Int. J. Mass Spectrom. Ion Process* **1987**, *78*, 53−68.

(35) Karas, M.; Bahr, U.; Hillenkamp, F. *Int. J. Mass Spectrom. Ion Process* **1989**, *92*, 231−242.

(36) Shin, S. K.; Han, S-J.; Kim, B. J. *J. Am. Soc. Mass Spectrom.* **1996**, *7*, 1018−1025.

(37) Shin, S. K.; Kim, B.; Haldeman, J. G.; Han, S-J. *J. Phys. Chem.* **1996**, *100*, 8280−8284.

(38) Anders, L. R.; Beauchamp, J. L.; Dunbar, R. C.; Baldeschwieler, J. D. *J. Chem. Phys.* **1966**, *45*, 1062−1063.

(39) Gioumousis, G.; Stevenson, D. P. *J. Chem. Phys.* **1958**, *29*, 294.
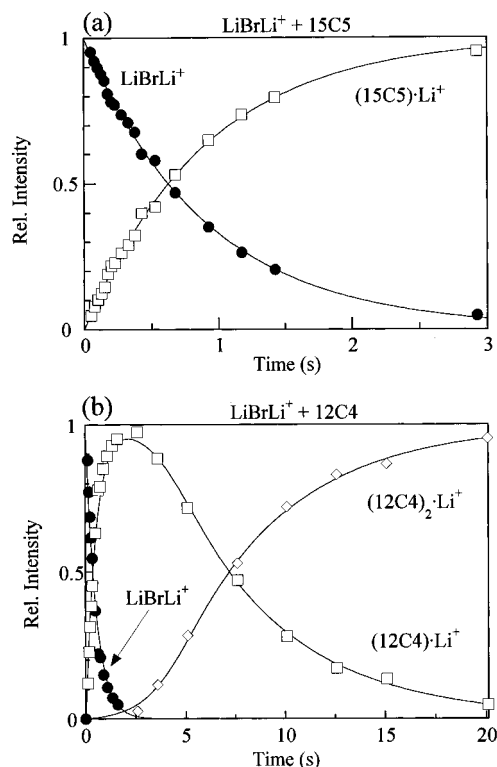
Figure 2. Reaction time plot of LiBrLi$^+$ with (a) 15-crown-5-ether at 2.1 × 10^{-8} Torr and (b) 12-crown-4-ether at 3.7 × 10^{-8} Torr. Solid lines are pseudo-first order fits to the data. Process 7 is included in the 12C4 data fit.

monitored as a function of time delay, and the results were simulated with pseudo-first-order reaction kinetics by a least-squares fitting program. Solvation energies were determined from the van't Hoff plot.[41,42]

The 308-nm output was from a XeCl excimer laser (Lambda-Physik, EMG-202 MSC), with a typical pulse width of ∼10 ns. The 3-mm-diameter laser beam was used unfocused to desorb lithium salt ions. Dibenzo-18-crown-6-ether absorbs at 308 nm. A typical laser power used in the desorption−ionization was ∼2 mJ.

All chemicals were purchased from Aldrich Inc. and were used after several freeze−pump−thaw cycles. The purity of each sample was tested by EI mass spectra. Sample inlet lines were baked and pumped out overnight to prevent cross-contamination between samples.

Computational Details. The geometry of the Li$^+$−Br$^-$−Li$^+$ triple ion was optimized at the Hartree−Fock (HF), second- and fourth-order Møller−Plesset perturbation theory[43] (MP2 and MP4) with a standard 6-311G(d, p) basis set[44] by use of GAUSSIAN-94 programs.[45] Vibrational frequencies were calculated at the HF level. The basis set superposition error was estimated at the MP2 level by using the full counterpoise method.[46] Geometries of monomeric complexes of Li$^+$ and LiBrLi$^+$ with 1,4-dioxane, 1,3-dioxane, and THF were optimized at the HF level with a standard 6-311G(d,p) basis set. Vibrational frequencies were calculated at the HF level. The binding energies were corrected for zero-point energies.

Results

Reactions of Li$^+$−Br$^-$−Li$^+$ with Crown Ethers. Reactions of LiBrLi$^+$ with 15-crown-5-ether are shown in Figure 2a. 15C5

(40) Meot-Ner, M. *J. Am. Chem. Soc.* **1983**, *105*, 4906−4911.
(41) Kebarle, P. *Annu. Rev. Phys. Chem.* **1977**, *28*, 445.
(42) Keese, R. G.; Castleman, A. W., Jr. *J. Phys. Chem. Ref. Data* **1986**, *15*, 1011.
(43) Moller, C.; Plesset, M. S. *Phys. Rev.* **1934**, *46*, 618−622.
(44) Krishnan, R.; Binkley, J. S.; Seeger, R.; Pople, J. A. *J. Chem. Phys.* **1980**, *72*, 650−654.
(45) Frisch, M. J. et al. *Gaussain 94, Revision C.2*; Gaussian, Inc.: Pittsburgh, PA, 1995.
(46) Boys, S. F.; Bernardi, F. *Mol. Phys.* **1970**, *19*, 553−566.

Table 1. Rate Constants for the Stepwise Solvations of LiBrLi$^+$ with Various O-Donors[a,b]

| | products | | | | | |
| | (S)$_n$·Li$^+$ | | (S)$_n$·LiBrLi$^+$ | | | |
S	$n = 1$	$n = 2$	$n = 1$	$n = 2$	$n = 3$	$n = 4$
15-crown-5-ether	17 ± 1					
12-crown-4-ether	20 ± 4	1.4 ± 0.3				
1,4-dioxane			0.20	0.62	0.056	
1,3-dioxane			0.30	0.90	0.40	
THF			0.15	1.21	0.057	0.014

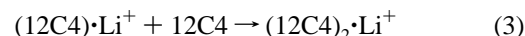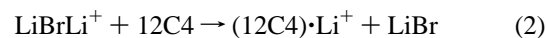[a] Rate constants are in units of 1.0 × 10^{-10} cm^3 molcule^{-1} s^{-1}. [b] Unless noted otherwise, errors are estimated at ±10%. Noted errors are the standard deviation of several experimental fittings. The accuracy of the absolute rates is estimated at ±25% due to the error in the pressure calibration.

abstracts Li$^+$ with a loss of LiBr. No 2:1 (15C5)$_2$·Li$^+$ complexes were detected.

$$\text{LiBrLi}^+ + 15\text{C5} \rightarrow (15\text{C5})\cdot\text{Li}^+ + \text{LiBr} \qquad (1)$$
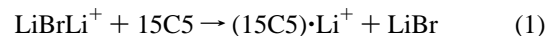
The rate constant for the formation of the 1:1 (15C5)·Li$^+$ complex was measured to be (17 ± 1) × 10^{-10} cm^3 molecule^{-1} s^{-1} (1.3 times the Langevin collision rate).[47,48] Table 1 summarizes the measured rate constants. The absence of the second solvation of Li$^+$ by 15C5 suggests that Li$^+$ is submersed into the cavity of 15-crown-5-ether.[28]
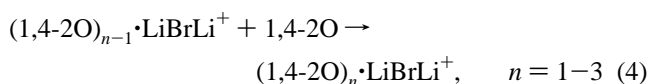
Reactions of LiBrLi$^+$ with 12-crown-4-ether are plotted in Figure 2b. Like 15C5, 12C4 abstracts Li$^+$ with a loss of LiBr. However, the reactivity of 12C4 differs from the reactivity of 15C5 in that (12C4)·Li$^+$ reacts again with 12C4 to form a (12C4)$_2$·Li$^+$ complex as reported by Chu et al.[28]

$$\text{LiBrLi}^+ + 12\text{C4} \rightarrow (12\text{C4})\cdot\text{Li}^+ + \text{LiBr} \qquad (2)$$

$$(12\text{C4})\cdot\text{Li}^+ + 12\text{C4} \rightarrow (12\text{C4})_2\cdot\text{Li}^+ \qquad (3)$$

The rate constant for the abstraction of Li$^+$ is (20 ± 4) × 10^{-10} cm^3 molecule^{-1} s^{-1}, while that for the second solvation is (1.4 ± 0.3) × 10^{-10} cm^3 molecule^{-1} s^{-1}. These solvation rates are 1.6 and 0.14 times the Langevin collision rate.[48] The second solvation rate is slower than the value of (3.6 ± 1.4) × 10^{-10} cm^3 molecule^{-1} s^{-1} reported by Chu et al.[28]

The abstraction of Li$^+$ by crown ethers is observed to have near unit efficiency compared with the Langevin collision rate constant. The loss of LiBr without forming the stable (crown ether)·LiBrLi$^+$ complexes indicates that the binding energies of Li$^+$ by 12C4 and 15C5 are much greater than the Li$^+$-BrLi bond dissociation energy of D_0(LiBr−Li$^+$) = 47 kcal mol^{-1} estimated at the MP4 level.

Solvations of Li$^+$−Br$^-$−Li$^+$ with Dioxanes. Figure 3a shows a time plot of reactions of LiBrLi$^+$ with 1,4-dioxane. LiBrLi$^+$ forms solvated complexes with 1,4-dioxane without losing LiBr. LiBrLi$^+$ was coordinated with up to three 1,4-dioxanes. No (1,4-2O)$_4$·LiBrLi$^+$ complexes were observed.

$$(1,4\text{-2O})_{n-1}\cdot\text{LiBrLi}^+ + 1,4\text{-2O} \rightarrow$$
$$(1,4\text{-2O})_n\cdot\text{LiBrLi}^+, \qquad n = 1\text{-3} \quad (4)$$

(47) It is known that Langevin collision theory underestimates ion−molecule collision rates with polar molecules (Su, T.; Bowers, M. T. *Gas Phase Ion Chemistry*; Bowers, M. T., Ed.; Acedemic: New York, 1979; Vol. 1, pp 83−118). This explains why some reaction rates are apparently faster than the Langevin collision rate.
(48) Polarizabilities of 12C4 and 15C5 were approximated as 2.0 and 2.5 times that of 1,4-dioxane (α = 8.60 Å^3 from: Stuart, H. A.; Schieszl, S. v. *Ann. Phys.* **1948**, *2*, 321).

10504   *J. Am. Chem. Soc., Vol. 119, No. 43, 1997*

Jarek and Shin
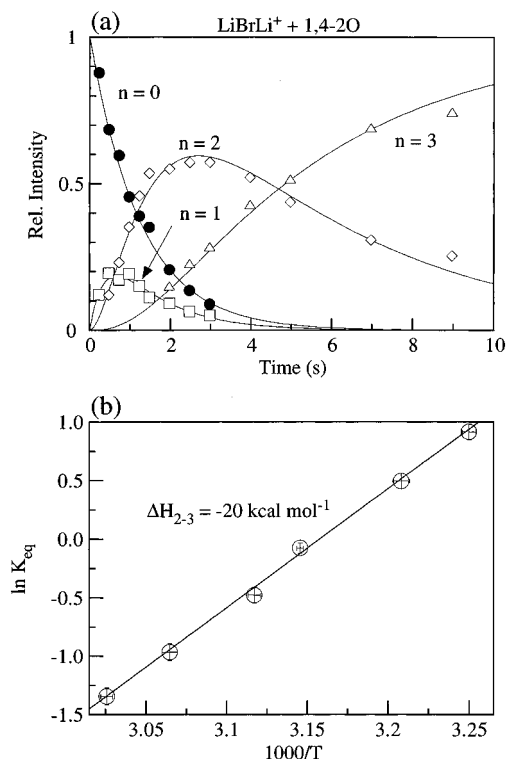
Figure 3. LiBrLi+ solvation with 1,4-dioxane: (a) reaction time plot at 1.3×10^{-6} Torr where solid lines are pseudo-first order fits to a consecutive irreversible kinetics scheme and (b) van't Hoff plot showing the temperature dependence of the equilibrium constants. The solid line represents a weighted linear-squares fit of the data.

The rate constants for the sequential solvations are 2.0×10^{-11}, 6.2×10^{-11}, and 0.56×10^{-11} cm^3 molecule^{-1} s^{-1} for $n = 1$, 2, and 3, respectively. The first solvation rate is only 0.02 times the Langevin collision rate. Collision-induced dissociation (CID) of $(1,4-2O)_2 \cdot LiBrLi^+$ in pure 1,4-dioxane yielded $(1,4-2O) \cdot LiBrLi^+$ with a loss of 1,4-dioxane. As the collision energy increases, $(1,4-2O) \cdot LiBrLi^+$ further dissociates to $LiBrLi^+$ with a loss of 1,4-dioxane. No $(1,4-2O)_n \cdot Li^+$ ($n = 1,2$) complexes were observed from CID. A gradual approach to thermal equilibria between $n = 2$ and 3 of $(1,4-2O)_n \cdot LiBrLi^+$ was evident at later times. The temperature dependence of the equilibrium constant was measured between $n = 2$ and 3. Figure 3b shows a van't Hoff plot. The slope represents the enthalpy change for the association of 1,4-dioxane to $(1,4-2O)_2 \cdot LiBrLi^+$. Thus, the binding energy of 1,4-dioxane to $(1,4-2O)_2 \cdot LiBrLi^+$ is determined to be 20 ± 2 kcal mol^{-1}, within a 95% confidence interval.

To see if the maximum coordination number and the binding energy varies with the O−O distance in bidentate ligands, reactions of $LiBrLi^+$ with 1,3-dioxane were examined. A reaction time plot is shown in Figure 4a. Similarly to 1,4-dioxane, $LiBrLi^+$ was solvated with up to three 1,3-dioxanes. No dissociative Li^+ solvation by 1,3-dioxane was observed.

$$(1,3-2O)_{n-1} \cdot LiBrLi^+ + 1,3-2O \rightarrow$$
$$(1,3-2O)_n \cdot LiBrLi^+, \qquad n = 1-3 \quad (5)$$
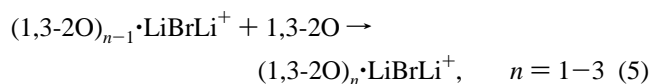
The rate constants for sequential solvations are 3.0×10^{-11}, 9.0×10^{-11}, and 4.0×10^{-11} cm^3 molecule^{-1} s^{-1} for $n = 1, 2$, and 3, respectively. The temperature dependence of the equilibrium constant between $n = 2$ and 3 is shown in Figure 4b. The slope yields a value of 23 ± 3 kcal mol^{-1} for the binding energy of 1,3-dioxane to $(1,3-2O)_2 \cdot LiBrLi^+$.
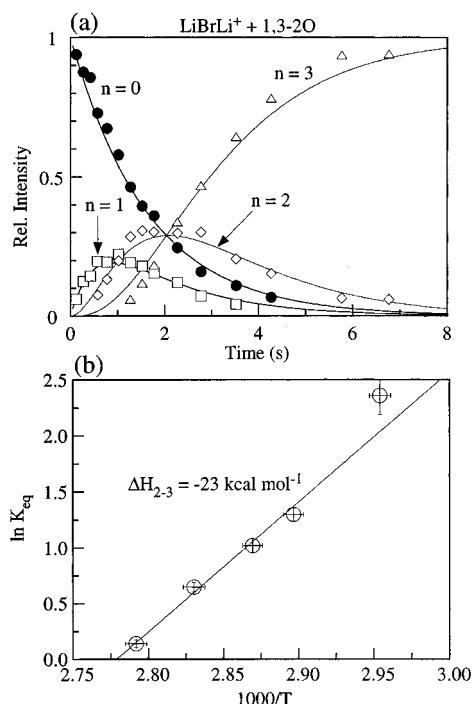

Figure 4. LiBrLi+ solvation with 1,3-dioxane: (a) reaction time plot at 6.3×10^{-7} Torr and (b) van't Hoff plot.
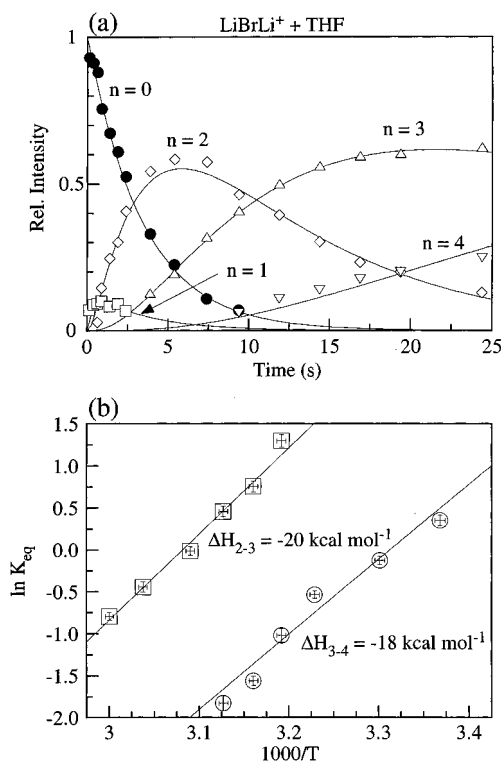
Figure 5. LiBrLi+ solvation with THF: (a) reaction time plot at 6.1×10^{-7} Torr and (b) van't Hoff plot.

Solvations of Li$^+$−Br$^-$−Li$^+$ with THF. A reaction time plot of $LiBrLi^+$ with THF is shown in Figure 5a. THF forms complexes with $LiBrLi^+$, but no dissociative Li^+ solvation is observed with THF. Up to four THFs are coordinated to $LiBrLi^+$.

$$(THF)_{n-1} \cdot LiBrLi^+ + THF \rightarrow$$
$$(THF)_n \cdot LiBrLi^+, \qquad n = 1-4 \quad (6)$$
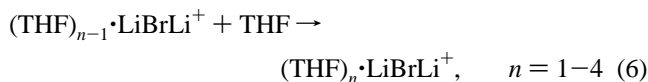
The rate constants for the sequential solvations are 1.49×10^{-11},

Table 2. Geometries, Vibrational Frequencies of LiBr and LiBrLi+, and the Bond Dissociation Energy of LiBrLi+ from *ab Initio* Calculations[a]

species	method	Li−Br (Å)	∠Li−Br−Li (deg)	ν[b] (cm−1)	D_0(Li+−BrLi) (kcal mol−1)
LiBr	HF	2.195		501	
	MP2	2.187			
	MP4(SDTQ)	2.187			
Li−Br−Li+	HF	2.321	180.0	379 (ν_1), 7.2 (ν_2), 388 (ν_3)	45.7
	MP2	2.313	153.6		47.3
	MP4(SDTQ)	2.311	152.4		47.4

[a] Basis sets are 6-311G(d,p). [b] Frequencies are scaled by dividing by 1.12.
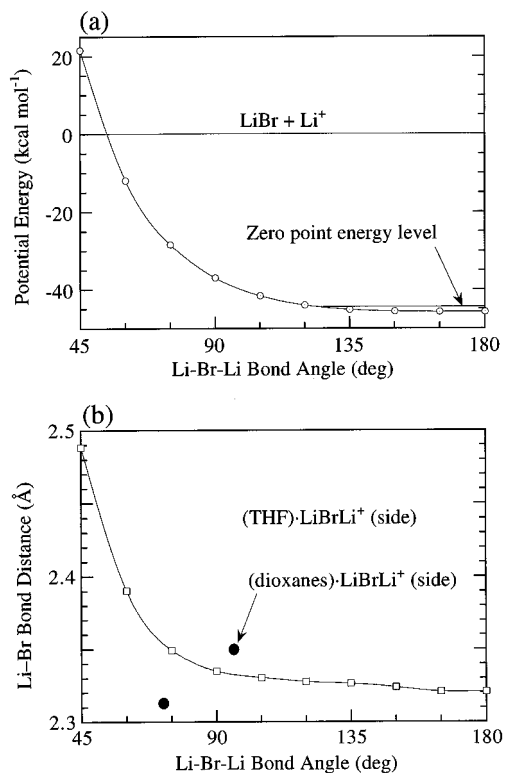
Figure 6. Potential energies and structures of LiBrLi+ at the HF/6-311G(d,p) level: (a) the adiabatic bending potential with the zero-point energy level and (b) the minimum energy Li−Br bond distance as a function of the Li−Br−Li bond angle.

12.14×10^{-11}, 0.57×10^{-11}, and 0.14×10^{-11} cm³ molecule^{-1} s^{-1} for $n = 1$, 2, 3, and 4, respectively. The fifth coordination of THF was not observed under the present experimental condition. A van't Hoff plot for thermal equilibria between $n = 2$ and 3 and between $n = 3$ and 4 is shown in Figure 5b. The binding energy of THF to (THF)$_2$·LiBrLi+ is determined to be 20 ± 2 kcal mol^{-1} and that to (THF)$_3$·LiBrLi+ is 18 ± 2 kcal mol^{-1}.

Theoretical Structures and Energetics of $Li^+−Br^−−Li^+$. The equilibrium geometry of LiBrLi+ varies with electron correlation, and the geometries are summarized in Table 2. HF predicts a linear equilibrium geometry of r(Li−Br) = 2.32 Å, whereas both MP2 and MP4 yield a bent geometry with r(Li−Br) = 2.31 Å and a bond angle of 153°. The energy difference between linear and bent geometries is only 20 cm^{-1} at the MP2 level. Figure 6 shows an adiabatic bending potential at the HF level and the Li−Br bond distance as a function of Li−Br−Li bond angle. As the bond angle decreases, the Li-Br bond distance increases. The zero-point energy level shown in Figure 6a illustrates the extreme floppiness of the bending potential. Though the equilibrium geometry is predicted to be bent, the vibrationally averaged structure is considered to be linear. The bond dissociation energy D_0(LiBr−Li+) was estimated to be
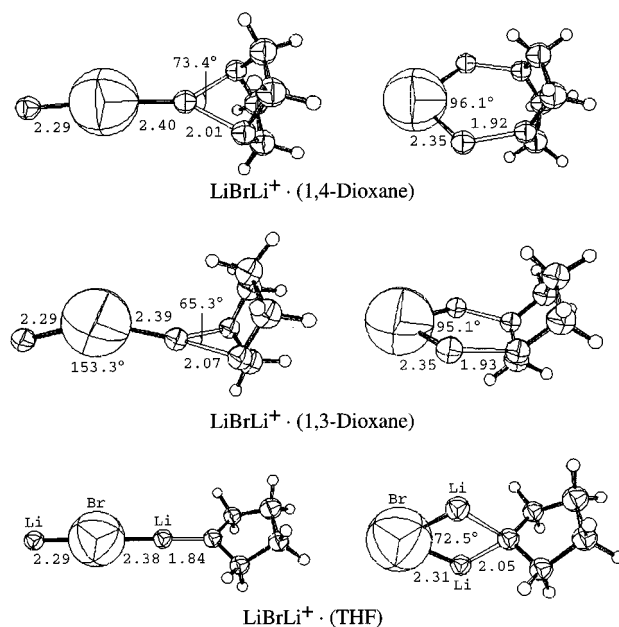
Figure 7. HF/6-311G(d,p) optimized structures of the 1:1 complexes of LiBrLi+ with 1,4-dioxane, 1,3-dioxane, and THF.

45.7 (HF), 47.3 (MP2), and 47.4 (MP4) kcal mol^{-1}. Correcting for the basis set superposition error decreases the binding energy by 0.7 kcal mol^{-1} at the MP2 level. The basis set deficiency error for the binding energy was estimated at the MP2 level with a 6-311G(3df,2pd) basis set. The extended basis set increased D_0(LiBr−Li+) by 0.1 kcal mol^{-1}. The HF value is in good agreement with both MP2 and MP4 estimates because the LiBr−Li+ bond cleavage involves a heterolytic partitioning of electrons to the ionic limit.

Structures and Energetics of 1:1 Complexes of Li+ and LiBrLi+ with Dioxanes and THF. Hartree−Fock optimized geometries of the 1:1 complexes of LiBrLi+ with 1,4-dioxane, 1,3-dioxane, and THF are shown in Figure 7. Table 3 summarizes selected geometrical parameters and relative energies. The structure of 1,4-dioxane in coordination complexes is assumed to have a twist-boat form with C_2 symmetry, whereas that of 1,3-dioxane is considered to have a chair form with C_s symmetry. Note that the boat form of 1,4-dioxane is 6.4 kcal mol^{-1} higher in energy than the chair form at the HF level. In the case of THF, the untwisted form with C_s symmetry is assumed for coordination. The untwisted form of THF lies 0.5 kcal mol^{-1} higher in energy than the twisted one with C_1 symmetry at the HF level.

Two coordination sites are considered in the 1:1 (S)·LiBrLi+ complex formation: the end-on and the side coordinations. The end-on complexes retain nearly linear LiBrLi+ geometries, while the side-coordination complexes contain bent LiBrLi+ geometries. In general, the end-on coordination elongates the nearest Li−Br bond from 2.32 Å in a free LiBrLi+ to ∼2.4 Å, while slightly contracting the other Li−Br bond to 2.29 Å. The side

Table 3. Geometries and Relative Energies of (S)·Li$^+$ and (S)·LiBrLi$^+$ at the HF Level with a 6-311G(d,p) Basis Set, Where S is 1,4-Dioxane (1,4-2O: Boat Conformation in C_2 Symmetry), 1,3-Dioxane (1,3-2O: Chair Conformation in C_s Symmetry), and Tetrahydrofuran (THF: Untwisted in C_s Symmetry)

species	O–O (Å)	O–Li (Å)	∠O–Li–O (deg)	Li–Br (Å)	∠Li–Br–Li (deg)	∠O–Li–Br (deg)	ZPE[a] (kcal mol^{-1})	ΔE (kcal mol^{-1})
1,4-2O (chair) + LiBrLi$^+$	2.775			2.321	180		74.5	0.0
1,4-2O (boat) + LiBrLi$^+$	2.658			2.321	180		74.4	6.4
(1,4-2O)·Li$^+$ + LiBr	2.397	1.952	75.7	2.195			75.8	6.1
(1,4-2O)·LiBrLi$^+$ (side)	2.532	1.915		2.347	96.1	117.3	76.9	−35.4
(1,4-2O)·LiBrLi$^+$ (end-on)	2.404	2.013	73.4	2.285, 2.399	176.7	143.2	76.0	−27.9
1,3-2O (chair) + LiBrLi$^+$	2.299			2.321	180		74.8	0.0
(1,3-2O)·Li$^+$ + LiBr	2.229	2.005	67.6	2.195			75.8	4.8
(1,3-2O)·LiBrLi$^+$ (side)	2.285	1.934		2.349	95.1	114.6	77.1	−39.4
(1,3-2O)·LiBrLi$^+$ (end-on)	2.235	2.072	65.3	2.292, 2.393	153.3	146.0	76.0	−30.8
THF (untwisted) + LiBrLi$^+$				2.321	180		70.8	0.0
(THF)·Li$^+$ + LiBr		1.795		2.195			71.8	2.3
(THF)·LiBrLi$^+$ (side)		2.053		2.313	72.5	102.0	72.7	−24.9
(THF)·LiBrLi$^+$ (end-on)		1.836		2.293, 2.381	178.3	179.9	72.1	−34.6

^{a} Frequencies are calculated at the Hartree−Fock level and scaled by 1/1.12.

coordination makes Li−Br−Li$^+$ bend to 96.1° with 1,4-dioxane, 95.1° with 1,3-dioxane, and 72.5° with THF. Geometries of (S)·Li$^+$ complexes with dioxanes and THF are comparable to those of the end-on (S)·LiBrLi$^+$ complexes.
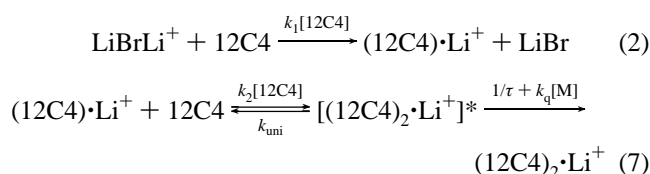
The binding energies are also included in Table 3 for 1:1 complexes of Li$^+$ and LiBrLi$^+$ with dioxanes and THF. The binding energies of 1:1 (S)·Li$^+$ complexes are calculated to be 40.4 kcal mol^{-1} for 1,4-dioxane (twist-boat), 42.4 kcal mol^{-1} for 1,3-dioxane (chair), and 44.1 kcal mol^{-1} for THF (untwisted). The Li$^+$ binding energy in (THF)·Li$^+$, calculated as 44.1 kcal mol^{-1}, is greater than the experimental value of 39 kcal mol^{-1} for (dimethyl ether)·Li$^+$,[30] but comparable to the value of 44 kcal mol^{-1} for (acetone)·Li$^+$.[27] The dissociative solvation channel to (S)·Li$^+$ + LiBr lies 2−5 kcal mol^{-1} higher in energy than the reactants LiBrLi$^+$ + S for the dioxanes and THF. This endothermicity explains the absence of 1:1 (S)·Li$^+$ complex formation with dioxanes and THF in the experiments. Between the end-on and the side coordination complexes, the latter species is more stable with dioxanes, while the former is more stable with THF. The side coordination of THF is not favored because it costs ∼19 kcal mol^{-1} in strain energy to bend LiBrLi$^+$. It is also interesting to see that the calculated binding energy of 34.7 kcal mol^{-1} in the end-on (THF)·LiBrLi$^+$ complex is greater than the bidentate interaction energies of end-on (dioxanes)·LiBrLi$^+$ complexes. These theoretical results suggest that the bidentate ligand prefers side coordination, whereas the monodentate ligand favors end-on coordination.

Discussion

Lifetime of the Ion−Molecule Collision Complex. Ion solvation in the gas phase differs from that in solution in that transient collision complexes formed by the charge-induced dipole interaction between the ion and the solvent undergo vibrational predissociation due to the lack of contacting bath molecules for the release of excess heat. In the first solvation of LiBrLi$^+$ with crown ethers the excess heat released from exothermic solvation of Li$^+$ induces a loss of LiBr. The association of the second solvent to (12C4)·Li$^+$ is mediated by ion−molecule collision complexes whose lifetimes depend strongly on the internal energy. When vibrationally hot (12C4)· Li$^+$ ions from the primary exothermic process encounter the second 12C4, they form collision complexes that predissociate rapidly. Association products cannot be readily formed until vibrationally hot (12C4)·Li$^+$ ions are thermalized by ligand-exchange and/or radiative relaxation processes.

The relaxation time delay between the formations of (12C4)· Li$^+$ and (12C4)$_2$·Li$^+$ was observed in pressure-dependence experiments. Figure 8 shows time plots of the reactions of LiBrLi$^+$ with 12C4 at the two partial pressures of 1.8×10^{-8} and 3.7×10^{-8} Torr. Symbols represent experimental data. A simple kinetics scheme that involves the [(12C4)$_2$·Li$^+$]* collision complex before the second solvation, eq 7, is introduced to fit experimental data.

$$\text{LiBrLi}^+ + \text{12C4} \xrightarrow{k_1[\text{12C4}]} (\text{12C4})\cdot\text{Li}^+ + \text{LiBr} \qquad (2)$$

$$(\text{12C4})\cdot\text{Li}^+ + \text{12C4} \underset{k_{uni}}{\overset{k_2[\text{12C4}]}{\rightleftharpoons}} [(\text{12C4})_2\cdot\text{Li}^+]^* \xrightarrow{1/\tau + k_q[\text{M}]}$$
$$(\text{12C4})_2\cdot\text{Li}^+ \quad (7)$$

k_1 and k_2 are the bimolecular reaction rate constants for the first and second solvations, respectively. k_{uni} is the rate constant for the unimolecular dissociation of the [(12C4)$_2$·Li$^+$]* collision complex, $1/\tau$ is the radiative relaxation rate, $k_q[\text{M}]$ is the rate of collisional quenching with background molecules, and [M] is the sum of [12C4] and [background molecules]. Since the ion−molecule collision rate constant is inversely proportional to the square root of the reduced mass, k_2 is taken to be $k_1(\mu/\mu')^{1/2}$, where μ and μ' are the reduced masses for processes 2 and 7, respectively. Analytical solutions assuming a constant value for k_{uni} lead to a poor fit of the experimental data, as shown in Figure 8 with dashed lines. To improve the fit, thermal relaxation of vibrationally hot (12C4)·Li$^+$ ions was considered by assuming a single exponential decay of k_{uni}.

$$k_{uni}(t) = k_{uni}(\infty) + [k_{uni}(0) - k_{uni}(\infty)] \exp^{-t/T} \qquad (8)$$

where $k_{uni}(0)$ and $k_{uni}(\infty)$ are the unimolecular dissociation rate constants for collision complexes of vibrationally hot (12C4)· Li$^+$ ions and those of thermalized (12C4)·Li$^+$ ions, respectively. T is a thermal relaxation time. Equation 8 is equivalent to the assmuption that the internal energy distribution of the collision complex, $f(E)$, relaxes exponentially to thermal equilibrium in eq 9.[49]

$$k_{uni}(t) = \int_{E_0}^{\infty} f_t(E) \frac{\rho(E)}{hN(E - E_0)} dE \qquad (9)$$

where

(49) Honovich, J. P.; Dunbar, R. C. *J. Am. Chem. Soc.* **1982**, *104*, 6220−6224.
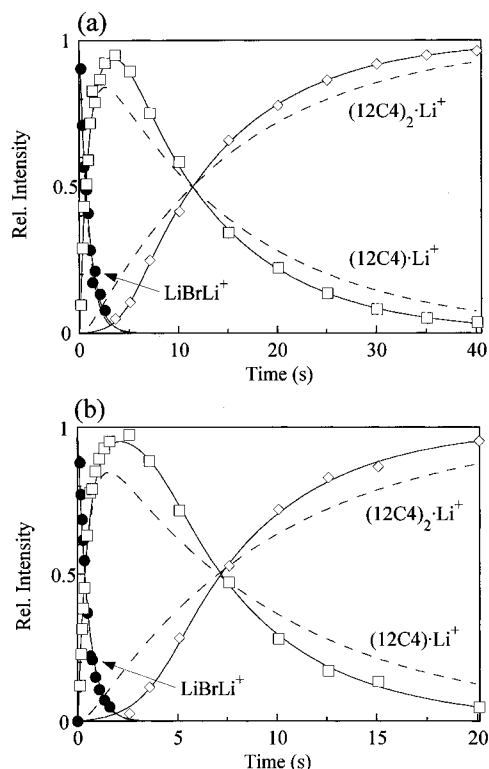
Figure 8. Reaction time plots of LiBrLi$^+$ with 12-crown-4-ether at (a) 1.8×10^{-8} and (b) 3.7×10^{-8} Torr. The solid curve fits include the formation of an intermediate collison complex, modeled by process 7, whereas dotted lines do not.

$$f_t(E) = f_{t=\infty}(E) + [f_{t=0}(E) - f_{t=\infty}(E)] \exp^{-t/T} \quad (10)$$

E is the internal energy, E_0 is a threshold for unimolecular dissociation, $\rho(E)$ is the density of states of the collision complex, h is Planck's constant, and $N(E - E_0)$ is the number of states of the transition state. Both $k_{uni}(0)$ and $k_{uni}(\infty)$ are independent of pressure, but the thermal relaxation time T varies with pressure. The solid curves in Figure 8 represent the best fit curves from the thermal relaxation model. The fitting parameters are $k_{uni}(0) = 540$ s^{-1}, $k_{uni}(\infty) = 5$ s^{-1}, and $T = 1.3$ s at 1.8×10^{-8} Torr and 1.1 s at 3.7×10^{-8} Torr. Values for $1/\tau + k_q[M]$ are 0.66 s^{-1} at 1.8×10^{-8} Torr and 0.79 s^{-1} at 3.7×10^{-8} Torr. The lifetime of the collision complex is estimated to be in the 2−200-ms range. As the pressure increases, the relaxation time T decreases but $1/\tau + k_q[M]$ increases. It appears that in the pressure range used in the present study bimolecular collisions play a significant role in forming association products by thermalizing vibrationally hot reactant ions via ligand-exchanging vibrational predissociation of collision complexes.

The Mechanisms of Stepwise Solvation of LiBrLi$^+$ by Dioxanes and THF. The temperature dependence of equilibrium constants yielded solvent binding energies from the slopes of van't Hoff plots. The binding energies for the third solvation are 23, 20, and 20 kcal mol^{-1} for 1,3-dioxane, 1,4-dioxane, and THF, respectively. Those for the first and second solvations are considered to be much greater than the third binding energy. That for the fourth coordination of THF is measured to be 18 kcal mol^{-1}, which is comparable to the third binding energy.

Solvations of LiBrLi$^+$ with dioxanes and THF provide interesting association kinetics exhibiting the effects of heat capacity, steric hindrance, and conformational change. The rate contstants for the successive solvations are plotted in Figure 9. Those for the first solvations are quite comparable to each other in the range $(0.15$ to $0.30) \times 10^{-10}$ cm^3 molecule^{-1} s^{-1}. The
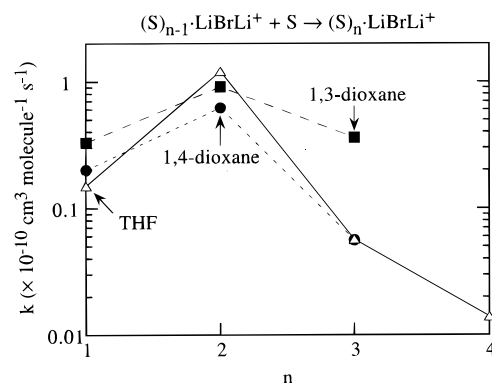
Figure 9. The rate constants for the stepwise solvations of LiBrLi$^+$ with 1,4-dioxane (circle), 1,3-dioxane (sqaure), and THF (triangle).

second solvation occurs 3−9 times faster than the first solvation in the range $(0.62$ to $1.21) \times 10^{-10}$ cm^3 molecule^{-1} s^{-1}. This increase in the apparent rate constant for the second solvation is ascribed to a decrease in k_{uni} of collision complexes. Note that the heat capacity increases in going from LiBrLi$^+$ to the 1:1 (S)·LiBrLi$^+$ complex. The decrease in rate constant for the third solvation is attributed to steric hindrance and a decrease in binding energy. Interestingly, the third solvation of 1,3-dioxane occurs about eight times faster than that for 1,4-dioxane, and the fourth coordination is absent in both 1,4- and 1,3-dioxanes. Meanwhile, the fourth solvation of THF is four times slower than the third solvation, most likely due to the steric effect because the binding energies for the third and fourth solvations are comparable to each other.

Theoretical energetics of the 1:1 complexes, the experimental kinetics, and the solvent-binding energies provide insight into the mechanism of stepwise solvation. The first step involves ligation of oxygen to one of the Li$^+$, most likely forming 1:1 end-on complexes due to the long-range charge-dipole interactions aligning Li$^+$ toward the oxygen atom(s). Thermal collision complexes then either predissociate to reactants or relax and rearrange to more stable association complexes. Theoretical energetics suggest that the most stable 1:1 complexes are side binding for dioxanes and end-on binding for THF. These differences in geometry of the 1:1 association complexes could affect the kinetics of the second solvation. In the (THF)·LiBrLi$^+$ end-on complex, one Li$^+$ site is coordinatively free, whereas in the (dioxane)·LiBrLi$^+$ side complexes, both lithiums are partially hindered by the preexisting ligand. The descending order of rate constants for the second solvation, k_2(THF) $>$ k_2(1,3-2O) $>$ k_2(1,4-2O), reflects such differences in steric hindrance.

The structure of the second solvation of LiBrLi$^+$ with dioxanes may have 1 end and 1 side coordination. The absence of the fourth coordination in dioxanes suggests that the Li$^+$ sites in the (dioxane)$_3$·LiBrLi$^+$ complex are coordinatively saturated with 2 end-bonded and 1 side-bonded dioxanes. The significant difference in rate constants for the third solvation between 1,3- and 1,4-dioxanes may be accounted for by considering the coordination geometry of dioxanes. The structure of 1,4-dioxane in bidentate coordination is considered to have a twist-boat form. Since the boat form of 1,4-dioxane is 6.4 kcal mol^{-1} higher in energy than the most stable chair conformation, the bidentate coordination of 1,4-dioxane involves conformational changes while forming coordination complexes. On the other hand, the coordination geometry of 1,3-dioxane is considered to have the most stable chair conformation. Unlike 1,4-dioxane, no conformational change is needed for the association of 1,3-dioxane. In fact, each stepwise solvation by 1,4-dioxane is slower than that by 1,3-dioxane due to the extra step involving conforma-

tional changes. In the case of THF, since the end-on coordination is the most stable structure, its complexes are considered to have the end-on structures of $(THF) \cdot LiBrLi \cdot (THF)^+$, $(THF)_2 \cdot LiBrLi \cdot (THF)^+$, and $(THF)_2 \cdot LiBrLi \cdot (THF)_2^+$ for the second, third, and fourth solvations, respectively.

Though ethers are commonly used as solvents in organolithium chemistry,[17] their complexes with lithium halides are rarely reported.[24,25,50−56] Li^+ is generally coordinated to a pseudotetrahedral geometry as in $[(LiCl)_2 \cdot (1,4\text{-}2O)_2]_\infty$,[51] $[LiCl \cdot 2THF]_2$,[52,53] $[2THF \cdot Li(\mu\text{-}(C_6H_4)_2(NH)N)(\mu\text{-}Cl)Li \cdot 2THF]$,[54] $[LiBr \cdot THF]_\infty$,[55] and $[LiBr \cdot Et_2O]_4$.[56] The five coordination is found in $[Li \cdot (MeOCH_2CH_2OMe)_2]Br$[24] and $[Li \cdot (12C4)]Cl$.[25] The proposed 2 end-coordination and 1 side-coordination structure of $(dioxanes)_3 \cdot LiBrLi^+$ has no precedence in the literature. The only reported dioxane structure in the solid state has 1 end-on coordination to each O in $[(LiCl)_2 \cdot (1,4\text{-}2O)_2]_\infty$,[51] where each Li is coordinated with two O and two Cl atoms. On the other hand, end-on structures similar to $(THF)_2 \cdot LiBrLi \cdot (THF)_2^+$ have been found in the solid state: $[LiCl \cdot 2THF]_2$[52,53] and $[2THF \cdot Li(\mu\text{-}(C_6H_4)_2(NH)N)(\mu\text{-}Cl)Li \cdot 2THF]$.[54]

Conclusion

The trapping of $Li^+ - Br^- - Li^+$ triple ions produced by MALDI in the ICR cell allows the kinetic studies of stepwise solvations of salt-bridge ions and the measurement of solvent-binding energy in the gas phase. In light of theoretical energetics and structures for 1:1 complexes of $LiBrLi^+$ with dioxanes and THF, the mechanisms of stepwise solvations are presented. In every step of solvation vibrational predissociation competes with the association processes. The association-to-predissociation branching ratio varies with the salt binding energy, solvent binding energy, heat capacity, steric hindrance, and conformational change of solvent. The relative populations of the solvated single ion, ion pairs, and triple ions will depend on solvent binding energies relative to the salt binding energy. When the solvent binding energy is greater than the salt binding energy, it leads to the dissociative solvation as exemplified in reactions of the $Li^+ - Br^- - Li^+$ triple ion with crown ethers. The excess heat released from the multidentate coordination of Li^+ by crown ethers causes the triple ion to dissociate instantaneously. This contrasts to the stepwise solvation observed with the other solvents, where no single step releases enough heat to effect the dissociation of the triple ion. Our result suggests that, in low dielectric constant solvents, the triple ion, once formed, will be a long-lived species that may be thermodynamically more stable than the solvated single ion or ion pair.

The FT-ICR/MALDI methodology presented herein for the $LiBrLi^+$ triple ion is generally applicable to other inorganic solid salt ions and allows the isolation and characterization of transient ionic intermediates that are present in conducting electrolyte solutions.

(50) Schmuck, A.; Leopold, D.; Wallenhauser, S.; Seppelt, K. *Chem. Ber.* **1990**, *123*, 761−799.

(51) Durant, F.; Gobillon, Y.; Piret, P.; van Meerssche, M. *Bull. Soc. Chim. Belg.* **1966**, *75*, 52.

(52) Hahn, F. E.; Rupprecht, S. *Z. Naturforsch.* **1991**, *46b*, 143−146.

(53) De Angelis, S.; Solari, E.; Gallo, E.; Floriani, C.; Chiesi-Villa, A.; Rizzdi, C. *Inorg. Chem.* **1992**, *31*, 2520−2527.

(54) Engelhardt, L. M.; Jacobson, G. E.; White, A. H.; Raston, C. L. *Inorg. Chem.* **1991**, *30*, 3978−3980.

(55) Edwards, A. J.; Paver, M. A.; Raithby, P. R.; Russell, C. A.; Wright, D. S. *J. Chem. Soc., Dalton Trans.* **1993**, 3265−3266.

(56) Neumann, F.; Hampel, F.; Schleyer, P. v. R. *Inorg. Chem.* **1995**, *34*, 6553−6555.